

Article

Effect of Fine Aggregate Gradation on Macro and Micro Properties of Cold Recycling Mixture Using Emulsified Asphalt

Zhigang Li ^{1,*} , Kexin Li ¹, Jianmin Zhang ², Ruibo Ren ^{1,*}, Pinru Du ³, Pinhui Zhao ¹ , Quanman Zhao ¹ 
and Litao Geng ¹

¹ School of Transportation Engineering, Shandong Jianzhu University, Jinan 250101, China; likexin5386@163.com (K.L.); zhaopinui08@163.com (P.Z.); zhaoquanman@sdjzu.edu.cn (Q.Z.); glt@sdjzu.edu.cn (L.G.)

² Shandong Luqiao Group Co., Ltd., Jinan 250101, China; zhangjm@sdluqiao.com

³ Shaanxi Transportation Holding Group Co., Ltd., Xi'an 710048, China; dupinru@126.com

* Correspondence: lizhigang@chd.edu.cn (Z.L.); rrbgq@sdjzu.edu.cn (R.R.)

Abstract: In order to explore the influence of fine aggregate on the macro and micro properties of cold recycling mixture using emulsified asphalt (CRME), mechanical and microscopic property tests were carried out. The indirect tensile strength (ITS), unconfined compressive strength (UCS) and triaxial shear strength of different fine aggregate gradation was measured for analyzing the effects of fine aggregate on the mechanical strength, triaxial shear resistance and fracture energy of CRME. Meanwhile, the surface morphologies and air voids distribution of different CRME were observed by scanning electron microscopy (SEM) and X-ray computed tomography (X-ray CT). The results show that fine aggregate has a significant effect on the mechanical strength and shear resistance of CRME. With the same water and asphalt content, the fracture energy and failure strain of the mixture with less fine aggregate (G3-2) decreased by 16.2% and 18.2%, respectively. The less content of powder there was, the fewer cement hydration products there were due to some cement being coated by emulsified asphalt and the “cement hydration products fiber” length being shorter. Approximately 70% of the Aft hydration products in the G3-2 mixture were in the range of 1–4 μm, while those in the G1 mixture were in the range of 4–8 μm. With the increase in filler content, the number of air voids in the volume range of $0.5 \text{ mm}^3 \leq V < 5 \text{ mm}^3$ in CRME decreased, and the number of air voids in the volume range of $V < 0.5 \text{ mm}^3$ significantly increased, while the equivalent radius of air voids decreased slightly with the increase in filler content.

Keywords: cold recycling mixture using emulsified asphalt; fine aggregate; macro and micro properties; surface morphologies; air voids distribution



Citation: Li, Z.; Li, K.; Zhang, J.; Ren, R.; Du, P.; Zhao, P.; Zhao, Q.; Geng, L. Effect of Fine Aggregate Gradation on Macro and Micro Properties of Cold Recycling Mixture Using Emulsified Asphalt. *Coatings* **2022**, *12*, 674. <https://doi.org/10.3390/coatings12050674>

Academic Editor: Valeria Vignali

Received: 14 April 2022

Accepted: 12 May 2022

Published: 14 May 2022

Publisher's Note: MDPI stays neutral with regard to jurisdictional claims in published maps and institutional affiliations.



Copyright: © 2022 by the authors. Licensee MDPI, Basel, Switzerland. This article is an open access article distributed under the terms and conditions of the Creative Commons Attribution (CC BY) license (<https://creativecommons.org/licenses/by/4.0/>).

1. Introduction

The recycling of waste materials has become the predominant way to realize green highways. Cold/hot recycling technology, rubber asphalt technology and the reutilization of construction waste or recycled plastic is applied and researched [1–4]. Due to the lack of aggregates, asphalt and other resources, and considering the energy conservation and environmental sustainability of pavement maintenance, emulsified asphalt cold recycling technology has been widely applied [5–7]. The void volume (VV) of CRME is generally 8%–13%, and few pavement diseases caused by air voids have been found when the VV is less than 8%. Early and long-term permanent deformation, loosening, water damage and other diseases are easy to occur when the VV is larger than 13%. Fine aggregate mainly fills the forming air voids between coarse aggregate, which is one of the most important factors affecting the VV of CRME. At the same time, fine aggregate gradation has a significant effect on the formation and distribution of emulsified asphalt mortar, thus affecting the macro performance of CRME. Therefore, it is of great significance to explore the influence

of fine aggregate gradation on the macro and micro properties of CRME for its material composition design and the improvement of its mechanical properties.

As machine-made sand content increases, the mechanical properties of CRME are also enhanced [8]. The contact angles and adhesive energy between the aggregates and asphalt significantly impact the water stability and fatigue performance of CRME [9], and the emulsified asphalt type has an appreciable effect on the adhesion between aggregates in a mixture [10]. In addition, intergranular mode fracture is the most common failure of mixtures for the weakness of the asphalt-aggregate interface [11]. Therefore, how to characterize the mortar interfacial characteristics of CRME is particularly important. Research work [12] studied the factors that affected the performance of CRME by macro and micro test methods. The stress dispersion state and cracking resistance mechanisms of mixtures were revealed through the micro interface. Generally, 1 wt.% ~1.5 wt.% cement is added to improve the early strength of CRME [13]. Meanwhile, high-temperature stability and water stability are also enhanced with increased cement addition [14]. With the increase in cement content, the low-temperature cracking resistance performance of cold recycled mixture did not decrease monotonically but presented a parabolic law [15]. That is, while the cement content was lower than 2%, the resistance to low-temperature cracking of the cold recycled mixture was enhanced as cement content increased. Pavement fracture toughness usually decreased with increasing percentages of RAP or decreasing cement content [16]. Cement that is not covered by emulsified asphalt completely hydrates with water in the mixture and forms a “three-dimensional space” structure by interweaving emulsified asphalt and cement hydration products. Furthermore, this three-dimensional space structure plays a “reinforcement” and “crack resistance” role in a mixture. The formed structure not only improved the strength of the mixture but also divided the air voids in the mixture, resulting in an increase in the number of air voids [17]. However, if part of the cement is covered by emulsified asphalt, the hydration reaction does not fully occur. Thus, this part of the cement is consistent with that of mineral powder [18,19]. Research pointed out that both low porosity and better coverage of aggregates could make the mixture show better performance [20]. Therefore, researchers had carried out a lot of research on the micro interface and void structure of CRME. The micro morphology and failure interface characteristics of CRME have been determined by X-ray CT scanning, SEM scanning and other micro testing methods combined with image processing, and it was found that the homogeneity of aggregate distribution, air void distribution and cement hydration products distribution is closely related to the macro mechanical strength of CRME [21–23]. The distributions of the air void parameters of cold recycled mixture and hot mix asphalt specimens along the specimen height are compared. It is found that the cold recycled mixture has more air voids and smaller diameters, while the HMA specimen has fewer voids and larger diameters. The change in the air void structure of cold recycled mixture is the fundamental reason for its strength attenuation [19]. There is a specific correlation between the distribution of air voids and the macro performance. How to evaluate the distribution characteristics of air voids in CRME has also attracted much attention. The Weibull statistical model can better reflect the distribution characteristics of air voids in cold recycled mixture [24]. At the same time, the performance of CRME can be prominently enhanced by adding fiber or waste materials [25].

At present, researchers mainly focus on the performance of CRME and have studied the influence of cement content, emulsified asphalt content, active filler type and fiber on the macro and micro performance of CRME. However, there is a lack of knowledge of the influence of fine aggregate gradation on the microstructure of a mixture, which could effectively provide theoretical support for the material composition design of CRME. It is necessary to know whether cement acts as an ordinary filler when ordinary fillers are insufficient. In this case, cement may not hydrate completely. Quantitative analysis of the cement hydration degree is also a difficult problem when ordinary filler is insufficient. Thus, this paper explores the influence of fine aggregate gradation on the macro mechanics, micro

interface morphology and air void structure characteristics of CRME through laboratory tests, providing theoretical support for the material design of CRME.

2. Materials and Methods

2.1. Materials

2.1.1. RAP and Raw Aggregates

In the design process of CRME, reclaimed asphalt pavement (RAP) aggregates are usually regarded as “black stone” without considering the influence of aged asphalt. The RAP used in this study was collected from the Qingdao Jiaozhou Bay Highway, and the sieving results are shown in Table 1. The asphalt was reclaimed by the Aberson method, and the testing results are listed in Table 2. The apparent relative density of manufactured sand was 2.721, the sand equivalent was 83% and the methylene blue value was 1.7 g/kg. The raw aggregates and RAP were sieved for subsequent testing.

Table 1. Results of sieving for RAP.

Sieve Size/mm	26.5	19	16	13.2	9.5	4.75	2.36	1.18	0.6	0.3	0.15	0.075
Passing Percentage/%	100	95.4	83.2	66.7	60.8	32.2	17.9	13.5	7.2	5.9	3.7	2.5

Table 2. Testing results of recycled asphalt from RAP.

Testing Index	Results
Penetration (25 °C; 0.1 mm)	32
Ductility (25 °C; cm)	61
Softening point (°C)	39.5

2.1.2. Emulsified Asphalt and Cement

Slow cracking and setting emulsified asphalt was prepared by using an Akzo Nobel emulsifier and Shell 70# asphalt. The main technical performance test results of emulsified asphalt and matrix asphalt are shown in Tables 3 and 4. In order to promote the demulsification of emulsified asphalt and increase the early strength of CRME, cement was added to CRME. However, cement has little effect on the long-term performance of a mixture [26,27]. Ordinary Portland cement was added with 1.5% content by mass according to the “Technical Specifications for Highway Asphalt Pavement Recycling” (JTG/T 5521-2019) [28], and all the technical specifications of the cement met the requirements of Specification JTG/T 5521-2019 [28].

Table 3. Test results of the technical performance of matrix asphalt.

Test	Results	Specification
25 °C penetration/0.1 mm	72	60~80
Softening point/°C	47	≥46
60 °C Dynamic viscosity/Pa·s	243	≥180
10 °C ductility/cm	63	≥20
15 °C Density/(g/cm ³)	1.012	Report
Wax content/%	1.5	≤2.2

Table 4. Test results of the technical performance of emulsified asphalt.

Test		Results	Specification
Emulsifying speed		Slow-Breaking	Slow or median Breaking
Ionic charge		Cationic (+)	Cationic (+)
Residue of 1.18 mm sieves/%		0.05	≤0.1
Evaporative residues	Residual content/%	62.8	≥62
	25 °C penetration/0.1 mm	83.2	50~300
	15 °C ductility/cm	47	≥40
Storage stability	1 day/%	0.6	≤1
	5 days/%	2.7	≤5

2.1.3. Mixture Design

In the gradation design, 80 wt.% RAP and 20 wt.% raw aggregate were used. In order to reduce the influence of material variation, the gradation of mixtures was accurately controlled by sieving. A mixture with fine aggregate grading coefficients (n_{FA}) of 0.4, 0.6 and 0.8 (G1, G2, G3 and G3-2), respectively, was designed, as shown in Table 5, based on the N method grading theory revised by A.N. Talbot. CRME was designed by the modified Marshall method according to Specification JTG/T 5521-2019 [28]. The optimum water content (OWC) of CRME was determined by the maximum dry density of the heavy hammer test with 4.0 wt.% emulsified asphalt content. The optimum emulsified asphalt content (mass ratio of emulsified asphalt to aggregates) was determined according to the wet and dry ITS (ITS_{dry}). The Marshall design results are shown in Table 6. In order to eliminate the influence of emulsified asphalt content on the test results, the control group G3-2 was set. Its grading was the same as that of G3, and other design information was identical to that of the G1 mixture, which is shown in Table 6.

Table 5. Gradations of the three types of CRME.

Sieve Size/mm	Passing Percent/%			Specification
	G1	G2	G3	
26.5	100	100	100	100
19	92.7	92.7	92.7	90~100
16	79.2	79.2	79.2	-
13.2	72.4	72.4	72.4	-
9.5	65.3	65.3	65.3	60~80
4.75	42.6	42.6	42.6	35~65
2.36	32.3	27.4	24.1	20~50
1.18	24.2	18.3	13.7	-
0.6	18.4	12.3	8.0	-
0.3	14.2	8.2	4.9	3~21
0.15	10.5	5.4	2.7	-
0.075	8.2	3.6	1.6	2~8
n_{FA}	0.4	0.6	0.8	-

Table 6. Mix design results of CRME.

Type of Mixture	Optimum Emulsified Asphalt Content/wt.%	Optimum Water Content/wt.%	Maximum Dry Density/(g/cm ³)	ITS _{dry} /MPa	Requirements of ITS _{dry} /MPa
G1	4.7	4.2	2.068	0.624	≥0.4
G2	3.9	3.8	2.010	0.563	≥0.4
G3	3.6	3.6	1.923	0.487	≥0.4
G3-2	4.7	4.2	1.907	0.537	≥0.4

2.2. Preparation of CRME Specimens

RAP, cement, water, emulsified asphalt and raw aggregate were prepared in a certain proportion, as mentioned above. Standard Marshall specimens were adopted for the ITS, UCS test and X-ray CT scanning test. Gyrotory Compacting specimens of 200 mm × 200 mm were made, and all the specimens were cured at 40 °C for 72 h in a constant temperature oven [29]. All of the specimens remained stationary at room temperature for 12 h after curing.

2.3. Experimental Method

2.3.1. Indirect Tensile Test

ITS was used for the mechanical properties of CRME, which reflected the cohesive properties of mixtures to a certain extent. At least four specimens were tested in each ITS test group, and the average value was calculated by the ITS results of four specimens. Before the test, the specimen was kept in a 15 °C constant-temperature water tank for 2 h, and the test loading rate was 50 mm/min.

2.3.2. Unconfined Compressive Strength

Due to the viscoelastic properties of asphalt mixture, it has significant temperature sensitivity [30]. In this study, UCS was adopted to characterize the carrying capacity of the mixtures. At least 6 h of heat preservation was required in a 25 °C incubator, with at least four specimens in each group. Testing was carried out by UTM-100 with a loading rate of 1 mm/min according to the “Standard Test Methods of Bitumen and Bituminous Mixtures for Highway Engineering” (JTG E20-2011) [31].

2.3.3. Triaxial Test

Specimens that were 100 mm in diameter and 200 mm in height were obtained by the drilling core test, and the top and bottom surfaces of the specimens were polished for the triaxial test. Before the triaxial test, the specimens were kept in a 25 °C incubator for at least 6 h. UTM-100 was used to carry out the triaxial test with a 3 mm/min loading rate [32]. Then, 50, 100 and 200 kPa were chosen as the confining pressures for the triaxial test, and at least three specimens were measured under each confining pressure. According to the calculation method of reference [32], the triaxial shear parameters of CRME were calculated. According to the stress-strain curve during the triaxial loading process, the fracture energy was calculated by integration. A schematic diagram of the calculation of the fracture energy and failure strain is shown in Figure 1.

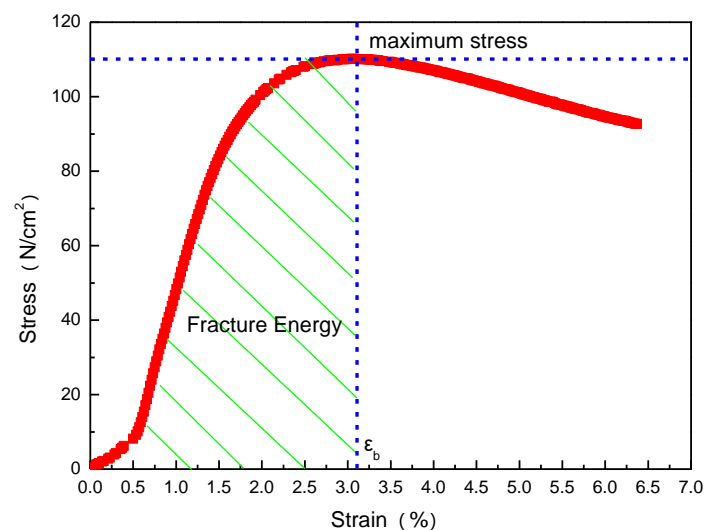


Figure 1. Calculation of fracture energy and failure strain.

2.3.4. Scanning Electron Microscopy Test

PHILIPS-FEI Quanta 200 SEM equipment was used to observe the micro-structure of the RAP aggregate at the ITS fracture interface. The micro-structure was observed to explore the influence of fine aggregate gradation on the spatial structure, which was an interweaving of emulsified asphalt mortar and cement hydration products in the mixture. The hydration products of AFt were quantitatively analyzed using Nano Measurer analysis software, and the hydration process of cement in the mixtures with different fine aggregate gradations was characterized by the length of AFt. Firstly, the standard length in the SEM image was calibrated, and then the length of the AFt needle was measured, as shown in Figure 2. After that, the distribution range of the AFt length was analyzed.

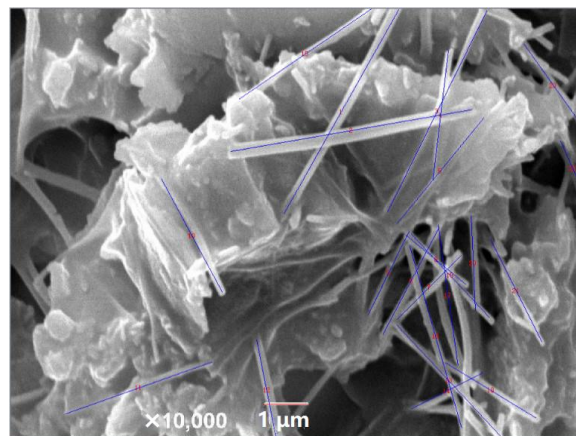


Figure 2. Nano Measurer statistical analysis for CRME (G1 mixture).

2.3.5. X-ray Computed Tomography Test

Y. Precision 225 kV X-ray CT with a scanning accuracy of two microns was adopted to determine the air void structure of the mixtures with different fine aggregate gradations. The optimum threshold value was determined by Otsu's algorithm, which is described in detail in article [24]. After three-dimensional scanning, VG software was used to reconstruct the air voids. The volume, surface area and position parameters of each air void in the mixtures were obtained, and all the information was used to explore the air void characteristics. Three image views and the three-dimensional reconstruction of the Marshall specimen after scanning are shown in Figure 3.

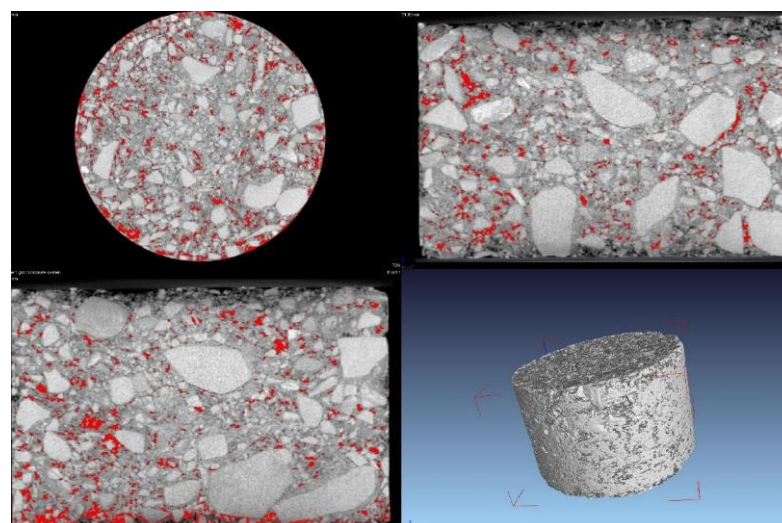


Figure 3. Three views and three-dimensional reconstruction image of a specimen.

3. Results and Discussion

3.1. Macro-Mechanical Properties of CRME

The results of the ITS and UCS are listed in Figure 4. The ITS and UCS of CRME decreased as the fine aggregate gradation coarsened. The UCS characterized the load-carrying capacity of CRME, which was related to the “inlay condition” of coarse aggregate. The greater the fine aggregate content was, the fuller the filling of air voids in the mixture was, and the mixture became denser, while the coarse aggregate had the same “inlay condition”. The distribution of air voids was more uniform, and the stress concentration was low, which showed that the ITS and UCS were relatively large. At the same time, the powder fillers used to form emulsified asphalt mortar were sufficient, and the cement was not required to act as a powder filler. In contrast, when the powder fillers were insufficient, some cement needed to be consumed to form emulsified asphalt mortar, which led to the cement hydration products decreasing. Meanwhile, the “reticulate spatial structure”, an interweaving of the cement hydration products and emulsified asphalt, became weakened, which resulted in the reduction of the macro-mechanical strength of CRME.

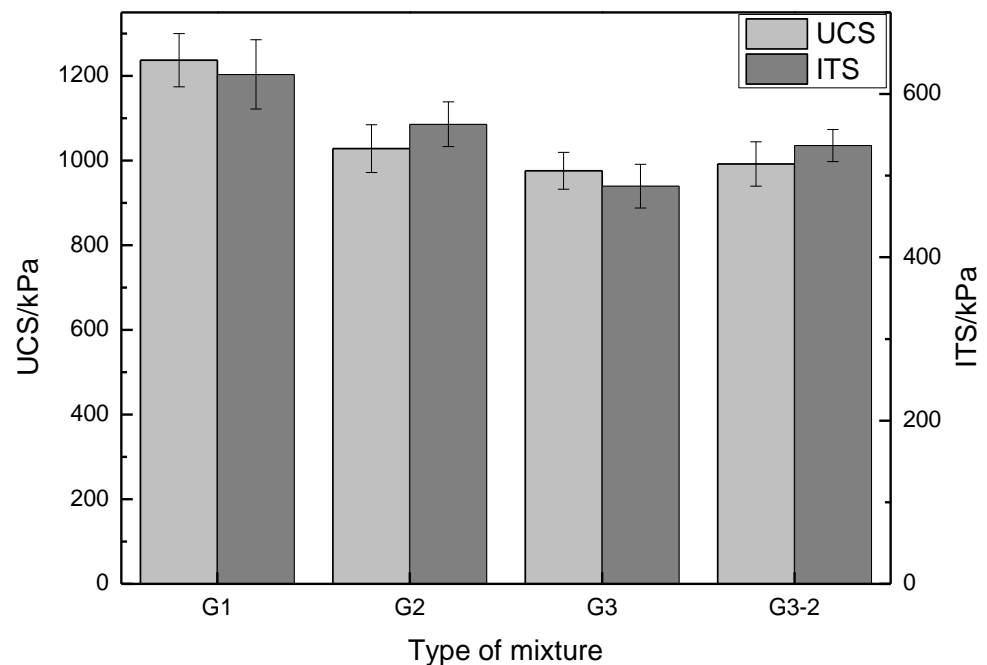


Figure 4. UCS and ITS results for the mixtures with different fine aggregate gradations.

The calculated results of the triaxial shear parameters, fracture energy and maximum failure strain are shown in Figure 5 and Table 7. According to the triaxial test results in Figure 5, as the fine aggregate gradation coarsened, the cohesion of CRME also decreased and the internal friction angle increased. Less effective filling occurred when the fine aggregate gradation coarsened. The adhesive effect of the emulsified asphalt mortar between the coarse aggregates decreased, which led to a decrease in the internal cohesion of CRME. On the contrary, due to the decreasing filler content, the emulsified asphalt content was reduced. This led to a strengthening of the “interlocked effect” between aggregates and a weakening of the “lubrication effect” of the emulsified asphalt. As a result, the internal friction angle of CRME increased.

In addition, the powder filler contents of the three gradations were quite different. Part of the cement was wrapped by emulsified asphalt due to the lower powder filler content, and the cement could not be fully used for hydration. The adhesion of the “network structure”, an interweaving of the cement hydration products and emulsified asphalt, decreased and resulted in the cohesion decrease of CRME. However, the cement hydration products had little effect on improving the “interlocked effect” between coarse aggregates,

and the internal friction angle of CRME mainly depended on the “interlocked condition” of the coarse aggregates themselves.

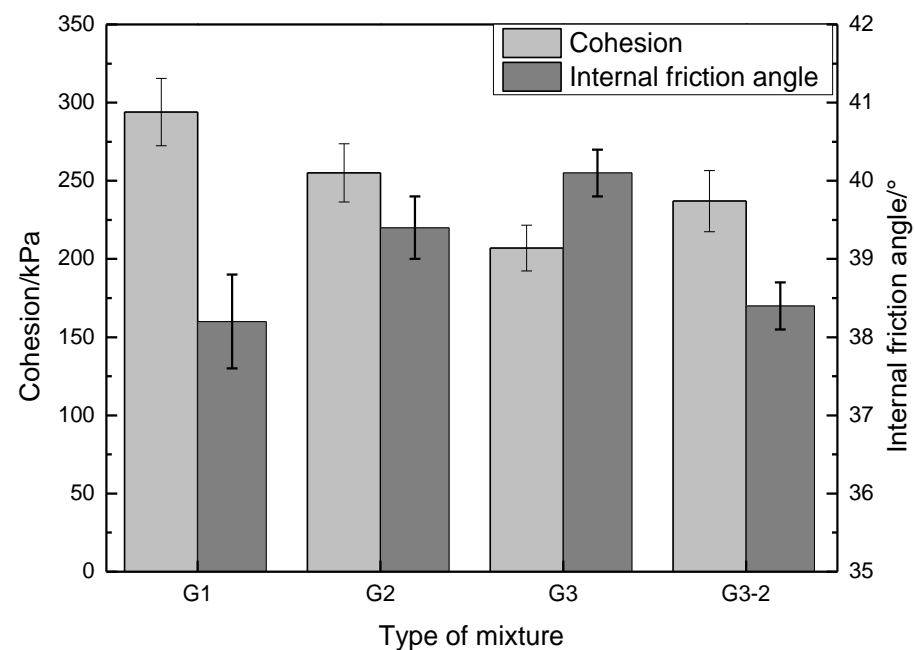


Figure 5. Triaxial test results for the mixtures with different fine aggregate gradations.

Table 7. Results of fracture energy and failure strain for the mixtures.

Type of Mixture	Confining Pressure 50 kPa		Confining Pressure 100 kPa		Confining Pressure 200 kPa	
	Fracture Energy/(N/cm ²)	Failure Strain/%	Fracture Energy/(N/cm ²)	Failure Strain/%	Fracture Energy/(N/cm ²)	Failure Strain/%
G1	247.6	4.6	322.7	4.4	462.3	3.8
G2	212.3	3.8	276.8	3.5	392.1	3.1
G3	173.4	3.0	242.5	2.6	354.2	2.3
G3-2	197.5	4.1	270.4	3.6	372.7	2.9

According to the test results in Table 7, as confining pressure increased, the fracture energy of CRME increased and the failure strain decreased. This indicated that confining pressure significantly improved the load-carrying capacity of CRME, and the triaxial test can better reflect the actual service state of pavement. With a decrease in filler content, both the fracture energy and failure strain of CRME decreased. Taking the test results of 100 kPa confining pressure as an example, compared with the G1 mixture, the fracture energy and failure strain of the G3 mixture decreased by 24.9% and 40.9%, respectively. Also compared with the G1 mixture, the fracture energy and failure strain of the G3-2 mixture decreased by 16.2% and 18.2%, respectively. It can be seen that the content of fine aggregate had a significant impact on the performance of CRME when compared with G1 and G3-2. The reason for this was that the lower the content of fine aggregates was, the lower the emulsified asphalt content was in the mixture, and the adhesion between the aggregates was weaker. Thus, less energy was needed to destroy the mixture. Similarly, as the emulsified asphalt mortar content decreased, the brittleness of CRME increased. Macroscopically, the failure strain was relatively small.

3.2. Microstructure Characteristics of the RAP Interface

Ordinary Portland cement is composed of gypsum and ground cement clinker, in which the cement clinker consists of C_3S , C_2S , C_3A , C_4AF , etc. The hydration process begins after the cement comes into contact with water. Then, hydration products such as calcium silicate hydrate (C-S-H), calcium hydroxide (CH) and Aft appeared. The air voids of CRME were filled and bridged by hydration products. Thus, a three-dimensional structure formed as the hydration products interweaved with emulsified asphalt mortar. Therefore, the quantity, shape and distribution of the hydration products have a great impact on the three-dimensional structure. However, C-S-H is mostly amorphous, and CH is in a layered structure. Both of them were difficult to quantify. Hence, in this paper, Aft was used for quantitative analysis to quantitatively describe the hydration product amounts.

As shown in Figure 6, there were a lot of cement hydration products and emulsified asphalt mortar on the RAP surface of the G1 mixture. The relatively smooth part in Figure 6 was emulsified asphalt mortar, while the needle-like and cluster structures were cement hydration products, namely, Aft and C-S-H, respectively. Aft and C-S-H interlaced with emulsified asphalt mortar resulted in the formation of a “network structure”. Furthermore, the “network structure” acted as a filler between the air voids in CRME. Aft and C-S-H extended into the emulsified asphalt mortar, forming an “anchorage structure”. The “bonding”, “reinforcement” and “crack resistance” effects between the aggregates were strengthened. The air void structure was segmented and filled due to the distribution of cement hydration products. This was the main reason that the strength of CRME was changed. In order to reveal the influence of fine aggregate gradation on the micro-structure of CRME, the differences in the micro-morphology of the aggregate surfaces of the G1, G3 and G3-2 mixtures were analyzed by SEM, as shown in Figure 7.

Figure 7a–c show the surface morphologies of the G1, G3 and G3-2 mixtures, respectively. Compared with Figure 7b, many more cluster C-S-H and needle-like Aft cement hydration products can be found in Figure 7a, and there were significantly fewer in Figure 7c. Owing to the large amount of fine aggregate in the G1 mixture, the powder filler content was relatively abundant. Sufficient powder filler was coated by emulsified asphalt forming mortar. By contrast, the amount of powder filler coated with emulsified asphalt forming mortar was insufficient. Emulsified asphalt needs to be further coated with cement to form a mortar. As a result, part of the cement played the role of powder filler and could not be completely hydrated due to asphalt coating. Hence, relatively few cement hydration products were observed.

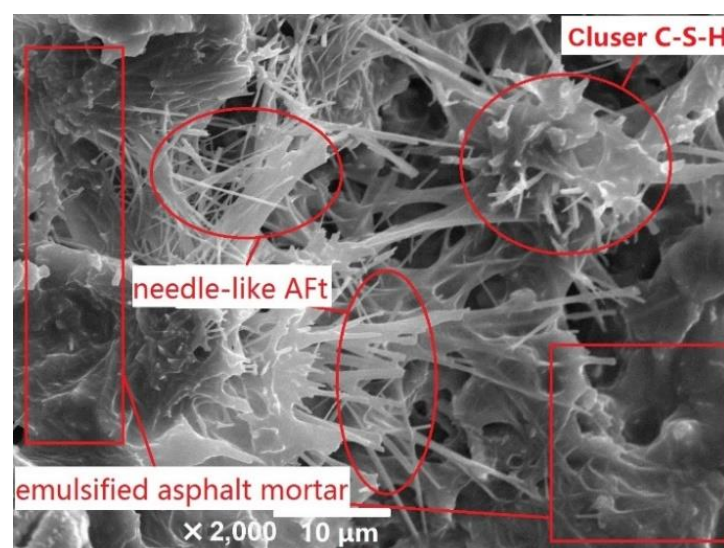


Figure 6. Interaction between the hydration products and asphalt mortar of the G1 mixture.

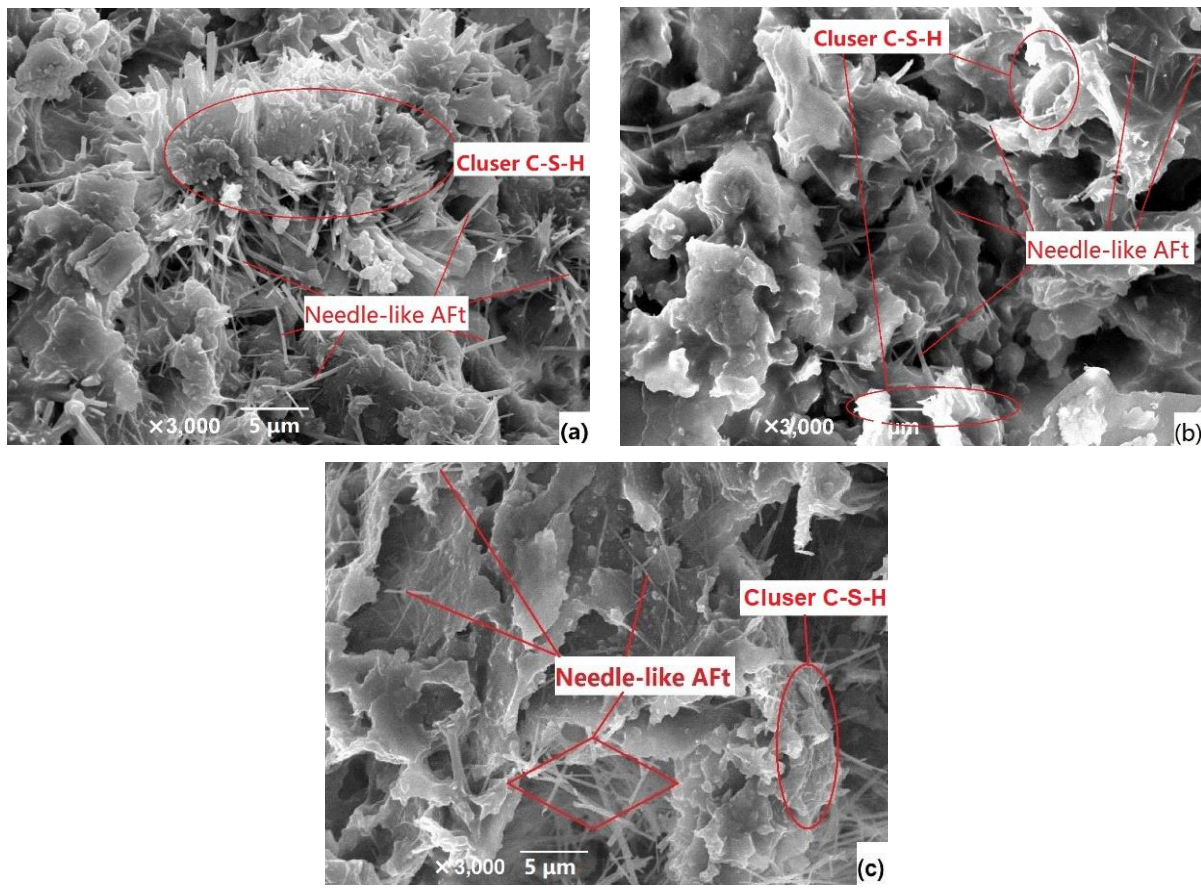


Figure 7. Morphology of aggregate surfaces of mixtures. (a) G1 mixture. (b) G3 mixture. (c) G3-2 mixture.

The length of the AFt hydration products in the G1, G3 and G3-2 mixtures was quantitatively analyzed using Nano Measurer software to evaluate the cement hydration degree.

According to the statistical results in Figure 8, 68.7% of the AFt hydration products in the G1 mixture were in the range of 4–8 μm , and 69.4% of the AFt hydration products in the G3 mixture were in the range of 2–5 μm , while 71.6% of the AFt hydration products in the G3-2 mixture were in the range of 1–4 μm . This indirectly showed that there were relatively more cement hydration products in the G1 mixture. It also was found that, as the cement content increased in CRME, the length of the AFt hydration products increased [18]. Therefore, this indicated that part of the cement in the G3 and G3-2 mixtures could not fully participate in the hydration reaction owing to the emulsified asphalt coating with cement (especially G3-2). At the same time, the longer the “AFt fiber” length of the hydration products was, the larger the interweaving area of the hydration products with emulsified asphalt was, and the “overlap effect” between the hydration products, the “embedding effect” into the aggregate surface and the “interweaving effect” with emulsified asphalt were all enhanced. The research results indicated that the quantity of cement hydration products and the interweaving state of asphalt and hydration products are the decisive factors of mixture performance [14]. However, fine aggregate gradation, especially the filler content, affected the composition of mortar in CRME. With the same emulsified asphalt content, the larger the proportion of the ordinary filler was, the less cement filler was used as ordinary filler, leading to an increase in the quantity of hydration products. Thus, the interfacial strength between the aggregate and emulsified asphalt mortar was enhanced, and the macroscopic strength of CRME was increased.

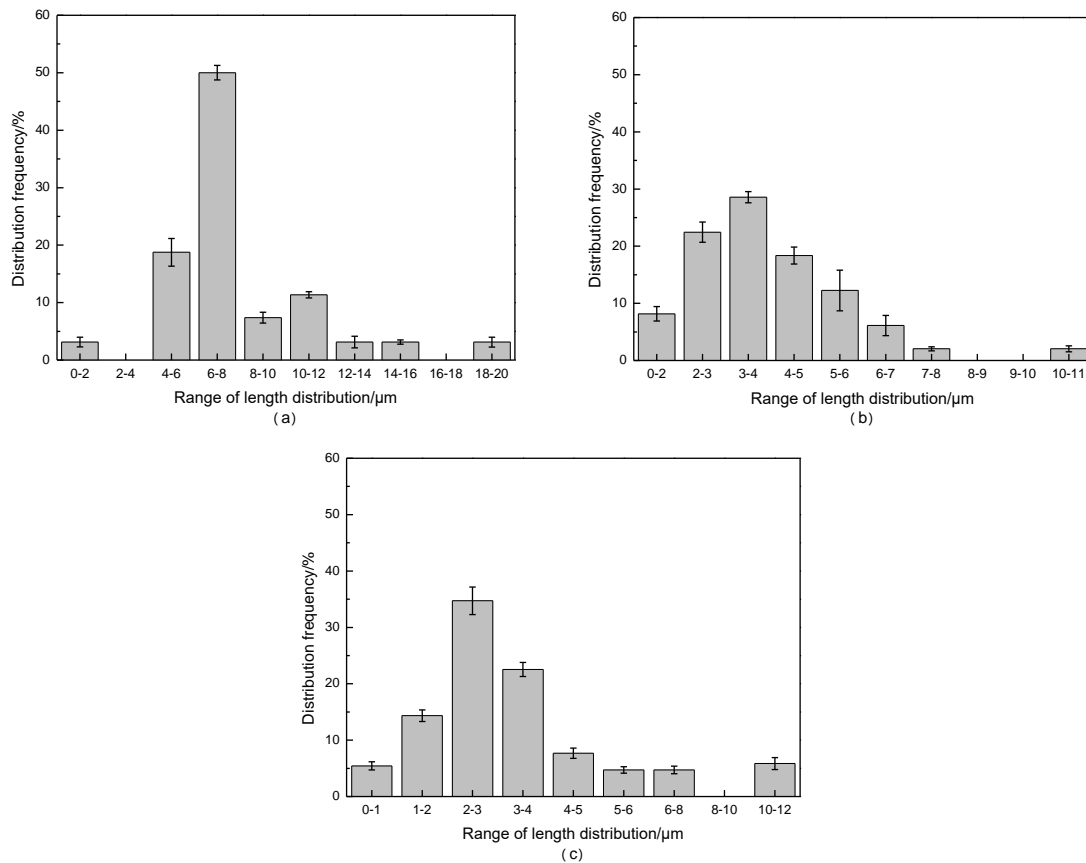


Figure 8. Quantitative analysis of cement hydration products distribution. (a) G1 mixture. (b) G3 mixture. (c) G3-2 mixture.

3.3. Air Void Structure Characteristics of CRME

3.3.1. Air Void Amount Distribution of CRME

According to the X-ray CT test results, the air void information (such as the amount, surface area, volume and three-dimensional position of each single air void) of CRME was obtained. The numbered percentage of air void amount was defined as the ratio of air voids in a certain volume range to the total air voids in CRME. The statistical results of the air void cumulative distribution in different mixtures are shown in Figure 9.

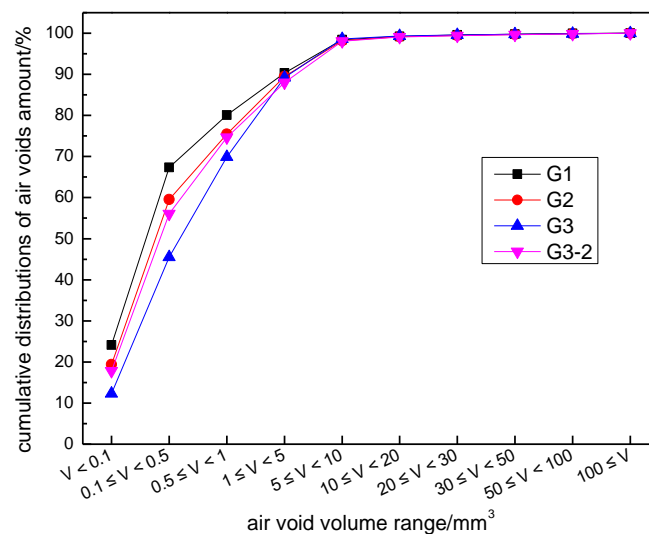


Figure 9. Cumulative distributions of air void amounts with different mixtures.

According to Figure 9, there was little difference in the distribution of air voids at a volume $V < 5 \text{ mm}^3$. However, with an increase in the filler content, the number of air voids in the volume range of $0.5 \text{ mm}^3 \leq V < 1 \text{ mm}^3$ and $1 \text{ mm}^3 \leq V < 5 \text{ mm}^3$ was reduced. On the contrary, the number of air voids increased in the volume range of $V < 0.5 \text{ mm}^3$. Compared with the G3 mixture, the number of air voids in the G1 mixture in the volume range of $0.5 \text{ mm}^3 \leq V < 5 \text{ mm}^3$ in CRME decreased by 47.4%; and that of G1 in the volume range of $V < 0.5 \text{ mm}^3$ increased by 48.0%. However, when compared with the G3-2 mixture, the number of air voids in the G1 mixture in the volume range of $0.5 \text{ mm}^3 \leq V < 5 \text{ mm}^3$ in CRME decreased by 27.9%; and that of G1 in the volume range of $V < 0.5 \text{ mm}^3$ increased by 20.1% (G1 and G3-2 had the same emulsified asphalt content). In other words, emulsified asphalt content and fine aggregate gradation both have significant effects on the distribution of air voids in CRME. On the one hand, the air voids of CRME were filled by redundant fine aggregate, and the original larger air voids were divided into several small-volume air voids. On the other hand, the higher the content of fine aggregate, the higher the content of emulsified asphalt required for coating aggregates. Larger volume air voids were filled and segmented by emulsified asphalt, which also led to a decrease in the number of large-volume air voids and an increase in the number of small-volume air voids in the mixture.

3.3.2. Equivalent Average Radius of Air Voids in CRME

Air voids were equivalent to a sphere of the same volume, and the radius of the sphere corresponding to the same volume as that of the air void was defined as the equivalent radius of the air voids. All equivalent radii of each air void in the mixture were averaged, and this was called the equivalent average radius. The equivalent average radius was used to describe the distribution characteristics of the air void size. The calculation method of the equivalent average radius is shown in Equation (1).

$$r = \frac{\sum_{i=1}^n \sqrt[3]{\frac{3V_i}{4\pi}}}{n} \quad (1)$$

where r is the equivalent average radius, mm; V_i is the volume of the air void numbered i , mm^3 ; n is the total number of air voids in the mixture.

All of the air voids of CRME were equivalent to spheres with the same volume. According to the CT scanning results and the calculation method, the equivalent average radius of the different mixtures was calculated, as shown in Table 8. The air voids were filled and divided into several small-volume voids as a result of a high content of fine aggregate and asphalt. Thus, the void volume and equivalent average radius were both small.

Table 8. Air void equivalent average radius of CRME with different gradations.

Type of Mixture	G1	G2	G3	G3-2
Equivalent average radius/mm	0.712	0.786	0.975	0.824

4. Conclusions

The influence of fine aggregate gradation on the mechanical properties, hydration products and air void structures were studied by macro and micro tests. The ultimate cause of the influence of fine aggregate gradation on the strength of CRME was revealed. However, the research will deeply explore the influence of air void morphology to find a relationship between the air void morphology parameters and mixture strength.

- (1) The content of fine aggregate had a significant effect on the ITS, UCS and shear strength of CRME. As the gradation of fine aggregate becomes finer, the emulsified asphalt content increased obviously. As a result, compared with the G1 mixture, the fracture energy and failure strain of the G3-2 mixture decreased by 16.2% and 18.2%, respectively (100 kPa).

- (2) Emulsified asphalt mortar and cement hydration products interweaved to form a “spatial network structure”, which had “reinforcement”, “anchorage”, “filling” and “crack resistance” effects. It was one of the most important factors for the strength formation of CRME.
- (3) While the powder filler was insufficient, part of the cement was coated with emulsified asphalt, which resulted in the cement failing to hydrate completely. Microscopically, fewer hydration products on the aggregate surface could be found with sufficient powder filler, while relatively more hydration products on the aggregate surface could be found with insufficient powder filler.
- (4) Quantitative analysis of the length of AFt hydration products was carried out. At about 70% distribution frequency, the length of the hydration products of the G1 mixture ranged from 4 to 8 μm , while that of the G3 and G3-2 mixtures ranged from 2 to 5 μm and 1 to 4 μm , respectively. Part of the cement in the G3 and G3-2 mixtures was not completely hydrated due to being coated with emulsified asphalt.
- (5) An increase in the filler content in fine aggregate resulted in an increase in the emulsified asphalt content in CRME. With the same emulsified asphalt content, when compared with the G3-2 mixture, the number of air voids in the G1 mixture in the volume range of $0.5 \text{ mm}^3 \leq V < 5 \text{ mm}^3$ in CRME decreased by 27.9%; and that of G1 in the volume range of $V < 0.5 \text{ mm}^3$ increased by 20.1%. Compared to the G3-2 and G1 mixtures, the equivalent radius of the air voids decreased by 13.4% with the increase in filler content.

The quantity, size and formation of the interweaving structure of cement hydration products and the number, distribution and size of the air voids were key to determining the performance of CRME. Therefore, in order to improve the performance of CRME, it is necessary to ensure the hydration quality of cement, increase the proportion of ordinary filler and improve the compaction effect to reduce the number of large volume air voids as much as possible.

Author Contributions: Conceptualization, Z.L. and R.R.; methodology, J.Z., K.L. and Z.L.; software, K.L.; formal analysis, K.L. and Q.Z.; investigation, K.L., P.Z. and Z.L.; resources, Z.L., P.D. and Q.Z.; data curation, Z.L. and K.L.; writing—original draft preparation, Z.L.; writing—review and editing, Z.L. and R.R.; visualization, K.L. and J.Z.; supervision, Z.L. and L.G.; project administration, Z.L.; funding acquisition, Z.L. and L.G. All authors have read and agreed to the published version of the manuscript.

Funding: This research was financially supported by the project ZR2020QE273 supported by the Shandong Provincial Natural Science Foundation, project ZR2020KE007 supported by the Key Program of Shandong Provincial Natural Science and project 2019KJG004 supported by the Shandong Provincial Young Scholars Innovative Research Team Development Program in Colleges and Universities.

Institutional Review Board Statement: Not applicable.

Informed Consent Statement: Not applicable.

Data Availability Statement: Using the data of this article requires approval from the authors.

Acknowledgments: We express our sincere gratitude to the experts, teachers and students who have provided help for this article.

Conflicts of Interest: The authors declare no conflict of interest.

References

1. Hamed, A.; Ahmad, A.B. Life cycle assessment of incorporating recycled materials in pavement design. *J. King Saud Univ. Eng. Sci.* **2022**, *in press*.
2. Fawaz, A.; Fahad, A.; Meshal, A.; Husnain, H.; Ahmed, E.; Sherif, E. Sustainability Evaluation of Cold In-Place Recycling and Hot Mix Asphalt Pavements: A Case of Qassim, Saudi Arabia. *Coatings* **2022**, *12*, 50.
3. Ruviano, S.A.; Silvestro, L.; Pelisser, F.; Azevedo, G.R.A.; Matos, R.P.; Gastaldini, G.L.A. Long-term effect of recycled aggregate on microstructure, mechanical properties, and CO₂ sequestration of rendering mortars. *Constr. Build. Mater.* **2022**, *321*, 126357. [[CrossRef](#)]

4. Ren, J.L.; Zhang, L.; Zhao, H.B.; Zhao, Z.D.; Wang, S.Y. Determination of the fatigue equation for the cement-stabilized cold recycled mixtures with road construction waste materials based on data-driven. *Int. J. Fatigue* **2022**, *158*, 106765. [[CrossRef](#)]
5. Turk, J.; Mauko, P.A.; Mladenovi, A. Cotič, Z.; Jurjavčič, P. Environmental comparison of two alternative road pavement rehabilitation techniques: Cold-in-place-recycling versus traditional reconstruction. *J. Clean. Prod.* **2016**, *121*, 45–55. [[CrossRef](#)]
6. Xu, J.Z.; Hao, P.W.; Zhang, D.P.; Yuan, G.A. Investigation of reclaimed asphalt pavement blending efficiency based on micro-mechanical properties of layered asphalt binders. *Constr. Build. Mater.* **2018**, *163*, 390–401. [[CrossRef](#)]
7. Iglesias, P.O.; Pasandín, A.M.R.; Pérez, I.P. Compaction and volumetric analysis of cold in-place recycled asphalt mixtures prepared using gyratory, static, and impact procedures. *Constr. Build. Mater.* **2021**, *296*, 123620.
8. Zarei, W.; Ouyang, J.; Yang, W.T.; Zhao, Y.Q. Experimental analysis of semi-flexible pavement by using an appropriate cement asphalt emulsion paste. *Constr. Build. Mater.* **2020**, *230*, 116994. [[CrossRef](#)]
9. Hou, Y.Q.; Ji, X.P.; Li, J.; Li, X.H. Adhesion between Asphalt and Recycled Concrete Aggregate and Its Impact on the Properties of Asphalt Mixture. *Materials* **2018**, *11*, 2528. [[CrossRef](#)]
10. Pan, C.L.; Liang, D.Q.; Mo, L.T.; Riar, M.; Lin, J.T. Influence of Different Modifiers on Bonding Strength and Rheological Performance of Bitumen Emulsion. *Materials* **2019**, *12*, 2414. [[CrossRef](#)]
11. Mubarak, M.; Osman, S.; Sallam, H.E.M. Effect of RAP content on flexural behavior and fracture toughness of flexible pavement. *Lat. Am. J. Solids Struct.* **2019**, *16*, e177. [[CrossRef](#)]
12. Lv, Z.H.; Shen, A.Q.; Qin, X.; Guo, Y.C.; Ruan, C.H. Performance Optimization and Mechanism of Emulsified Asphalt Cold Recycled Mixtures. *J. Build. Mater.* **2018**, *21*, 90–95.
13. Lin, J.T.; Wei, T.Z.; Hong, J.X.; Zhao, Y.L.; Liu, J.P. Research on development mechanism of early-stage strength for cold recycled asphalt mixture using emulsion asphalt. *Constr. Build. Mater.* **2015**, *99*, 137–142. [[CrossRef](#)]
14. Yang, Y.H.; Yang, Y.; Qian, B.T. Performance and Microstructure of Cold Recycled Mixes Using Asphalt Emulsion with Different Contents of Cement. *Materials* **2019**, *12*, 2548. [[CrossRef](#)] [[PubMed](#)]
15. Xu, J.Z.; Hao, P.W.; Wang, H.; He, L.J. Influences of two binder materials on performance of cold recycled mixtures stabilized with foamed asphalt. *Acta Mater. Compos. Sinica* **2017**, *34*, 687–693.
16. Mubarak, M.; Sallam, H.E.M. Reliability study on fracture and fatigue behavior of pavement materials using SCB specimen. *Int. J. Pavement Eng.* **2018**, *21*, 1563–1575. [[CrossRef](#)]
17. Wang, H. Meso-microscopic Void Distribution Characteristics of Emulsified Asphalt Cold Recycled Mixture with Different Cement Contents. *J. Highw. Transp. Res. Dev.* **2016**, *33*, 27–34.
18. Li, Z.G.; Hao, P.W.; Xu, J.Z. Study on Impacts of Freeze-thaw Cycles on the Shear Performances of Emulsified Asphalt Cold Recycle Mixture. *Mater. Rev.* **2016**, *30*, 121–125.
19. Li, Z.G.; Hao, P.W.; Liu, H.Y.; Xu, J.Z. Effect of cement on the strength and microcosmic characteristics of cold recycled mixtures using foamed asphalt. *J. Cleaner Prod.* **2019**, *230*, 956–965. [[CrossRef](#)]
20. Bahiense, A.V.; Alexandre, J.; Xavier, G.; Azevedo, G.R.A.; Monteiro, N.S. Dosage of interlocking paving with ornamental rock waste: An experimental design approach, particle packing and polluting potential. *Case Stud. Constr. Mater.* **2021**, *15*, e00596.
21. Lyu, Z.H.; Shen, A.Q.; Qin, X.; Yang, X.L.; Li, Y. Grey target optimization and the mechanism of cold recycled asphalt mixture with comprehensive performance. *Constr. Build. Mater.* **2019**, *198*, 269–277. [[CrossRef](#)]
22. Omrani, M.A.; Modarres, A. Stiffness and Fatigue Behavior of Emulsified Cold Recycled Mixture Containing Waste Powder Additives: Mechanical and Microstructural Analysis. *J. Mater. Civ. Eng.* **2019**, *3*, 04019061. [[CrossRef](#)]
23. Gao, L.; Wang, Z.Q.; Liu, Y.P.; Zheng, J.Q.; Li, H. Influence of Binder Property and Mortar Thickness on High-Temperature Performance of Cold Recycled Mixtures with Asphalt Emulsion. *Materials* **2019**, *12*, 2718. [[CrossRef](#)] [[PubMed](#)]
24. Gao, L.; Ni, F.; Luo, H.L.; Charmot, S. Characterization of air voids in cold in-place recycling mixtures using X-ray computed tomography. *Constr. Build. Mater.* **2015**, *84*, 429–436. [[CrossRef](#)]
25. Sun, J.X.; Liu, L.P.; Sun, L.J. Effect of fiber on fatigue performance of emulsified asphalt cold recycled mixture. *J. Wuhan Univ. Technol. (Transp. Sci. Eng.)* **2019**, *43*, 97–101.
26. Li, Z.G.; Hao, P.W.; Liu, H.Y.; Xu, J.Z. Investigation of early-stage strength for cold recycled asphalt mixture using foamed asphalt. *Constr. Build. Mater.* **2016**, *127*, 410–417. [[CrossRef](#)]
27. Lin, J.T.; Huo, L.; Xu, F.; Xiao, Y.; Hong, J.X. Development of microstructure and early-stage strength for 100% cold recycled asphalt mixture treated with emulsion and cement. *Constr. Build. Mater.* **2018**, *189*, 924–933. [[CrossRef](#)]
28. *JTG/T 5521-2019; Technical Specifications for Highway Asphalt Pavement Recycling*. Ministry of Transport of the People's Republic of China: Beijing, China, 2019.
29. Li, Z.G.; Hao, P.W. Effect of curing procedure to foamed asphalt cold recycled mixture properties. *J. Beijing Univ. Technol.* **2016**, *42*, 79–85.
30. Lytton, R.L.; Zhang, Y.; Gu, F.; Luo, X. Characteristics of damaged asphalt mixtures in tension and compression. *Int. J. Pavement Eng.* **2018**, *19*, 292–306. [[CrossRef](#)]
31. *JTG E20-2011; Standard Test Methods of Bitumen and Bituminous Mixtures for Highway Engineering*. Ministry of Transport of the People's Republic of China: Beijing, China, 2011.
32. Jenkins, K.J.; Collings, D.C. Mix design of bitumen-stabilised materials—South Africa and abroad. *Road Mater. Pavement Des.* **2017**, *18*, 331–349. [[CrossRef](#)]